Phase transitions in ferroelectric-paraelectric superlattices

A. P. Levanyuk[1, 2, 3] and I. B. Misirlioglu[1]

[1] *Faculty of Engineering and Natural Sciences, Sabanci University, Tuzla/Orhanli, 34956, Istanbul, Turkey*

[2] *Moscow Institute of Radioengineering, Electronics and Automation, Moscow 117454, Russia*

[3] *Departamento de Fisica de la Materia Condensada, C-III, Universidad Autonoma de Madrid, 28049 Madrid, Spain*

Abstract

Within the phenomenological Landau-Ginzburg-Devonshire theory we discuss the paraelectric-ferrolectric transition in superstructures consisting of ferroelectric and paraelectric layers of equal thickness. The polar axis of the ferroelectric is perpendicular to the layer plane that is similar to what is expected on fully strained $BaTiO_3/SrTiO_3$ superstructures on $SrTiO_3$ substrates with pseudomorphic electrodes. We concentrate on the electrostatic effects and do not take into account the boundary conditions other than the electrostatic ones. We find that when the ferroelectric phase transition in the superstructures is into a multidomain state, both its temperature and its character, i.e. the profile of the polarization appearing at the phase transition is strongly influenced by the nature of the near-electrode region. This is also the case for the layer thickness separating the single- and multidomain regimes of the transition. This finding makes us question the idea of infinite system, i.e. the system where boundaries of the sample are neglected, and periodic superstructures similar to a crystal. The irrelevance of this idea in certain conditions is demonstrated by comparing the phase transitions in two different superstructures consisting of ferroelectric and paraelectric layers of the same thickness. In one of them the ferroelectric layer is in immediate contact with ideal metallic electrode while at the other boundary it is a paraelectric layer which is in the contact with the electrode. In another superstructure, one paraelectric layer is splitted in two equal parts which are placed as the first and last layer between the electrodes and the ferroelectric layers which are closest to the electrodes. We show (with some formal reservations) that the phase transition temperature in the first superstructure can be over 100 °C more than in the second one if the material parameters of $BaTiO_3/SrTiO_3$ are used for the estimations. Moreover, the profile of the polarization arising at the phase transition is inhomogeneous along the superstructure and has the maximum amplitude in the ferroelectric layer contacting the electrode. We argue that this situation is general and results in smearing of the phase transition anomalies for the layer thicknesses corresponding to multidomain transitions. The work is mainly analyical but numerical methods has been used to support some statements which have been put forward as hypothesis.

I. INTRODUCTION

There is a lot of attention devoted now to ferroelectric-paraelectric superlattices [1–3]. However the phenomenological theory of phase transitions in these systems is still far from being complete and consistent. This may seem surprising because the theory of these systems started [4–7] well before the first experimental realization of the superlattices [8–9]. A general feature of the theoretical works was an assumption that the ferroelectric polarization was parallel to the plane of the structure. This was both natural and correct because the authors considered superlattices containing layers of cubic ferroelectics with the layer plane perpendicular to a cubic axis. It was correct to expect that the ferroelectic polarization would be directed along a cubic axis parallel to the layer plane because there was no depolarizing field in this situation. However, the experimentally realizable multilayers do not consist of cubic ferroelectric materials. Because of the misfit strains, the cubic paraelectric phase converts into (at least) tetragonal either with the polar axis perpendicular either to the layer plane (uniaxial ferroelectric) or with two polar axes parallel to the plane (two-axial ferroelectric). In this paper we are concerned with the former, uniaxial case which seems to be the main interest for experimental works. Since the ferroelectric polarization is perpendicular to the interface the depolarizing field takes on the leading role in defining both the temperature and the character of the ferroelectric phase transition and the non-electrostatic boundary conditions at the interface ("short-range interlayer interaction") which were the main topic of Refs. 4-7 become of secondary importance. This reasonable idea was pursued in Refs. 10-11 where the authors discussed one aspect of the depolarizing field: Lowering of the temperature of the ferroelectric phase transition into the single domain state, which is an effect known, in principle, since the work of Batra *et al.* [12]. In other words, the authors took for granted that the ferroelectric phase transition is a transition into a single domain state. However, that this transition could be into a multidomain state is another possibility. It should be noted that the interplay between a single- and multidomain transitions in a system quite similar to multilayers, specifically, in a ferroelectric slab between metallic electrodes and two dielectric layers between the ferroelectric and the electrodes has been discussed to some detail by Chensky and Tarasenko (ChT) [13] in their 1982 paper. The approach of ChT has been used by Stephanovich *et al.* [14] to discuss the ferroelectric phase transitions in multilayers of the type we are concerned with. In their work, they supposed that the space

distribution of the ferroelectric polarization appearing as a result of the phase transition is periodic along the superstructure. This analogy with ordinary crystal looks quite natural and it is not surprising that other research groups have adopted this assumption [14,15]. Nevertheless, using the same approach as in Ref. 14 we show that the periodicity assumption along the thickness is not justified. We consider two specific cases of superstructures. For one of them we explicitly show that the assumption of periodicity does not hold regardless of the system size. For another special case the assumption of periodicity seems to be, hypothetically, correct but this system is very specific. Considering a general case, we can put forward physical arguments only but they are not in favor of the use of periodicity along the thickness of the system when the transition is into a multidomain state.

The physical reason for the lack of the periodicity is that the superstructure is never sufficiently long to consider it as an analog of a periodic crystal. Experimentally, the lateral sizes of the electrode or external surface are always much larger than the total thickness of the superstructure. Theoretically, this corresponds to the supposition that the layers are laterally infinite. Therefore, no point or region inside of the superstructure is "sufficiently far" from the boundaries. At the same time, the structure of the boundary layers defines to a considerable extent how the depolarizing field is screened (if at all) from the exterior and this influences the whole system. To show this, we compare the phase transitions in two different superstructures consisting of ferroelectric and paraelectric layers of the same thickness. In one of them the ferroelectric layer is in immediate contact with ideal metallic electrode while at the other boundary it is a paraelectric layer which is in the contact with the electrode, namely a bilayer cell. In the other superstructure, one paraelectric layer is splitted in two equal parts which are situated between the electrodes and ferroelectric layers. We were unable to rigorously analyze the phase transitions in the two systems. However, we were able to show that the phase transitions are very different both in terms of the transition temperatures and the profile of the space distribution of ferroelectric polarization arising at the transition.

The demonstrated sensitivity of the phase transition to the characteristics of the near-electrode region forces us to be cautious about comparison of the experimental data with theoretical formulas for idealized models of the type we are considering in this paper. That is why we do not try to make this comparison though, for the sake of illustration, we use in our plots the physical parameters of $BaTiO_3$-$SrTiO_3$ superstructures. To our understanding,

to be relevant to the experiment, the theory should take on further developments and we consider our paper as no more than a step in this direction. This paper raises questions rather than giving answers: We emphasize uncertainties in our results for different considerations and difficulties which we met when trying to treat even idealized systems consistently.

Throughout the paper we shall not take into account the non-electrostatic boundary conditions at the ferroelectric-paraelectric interfaces, similar to ChT [13] and unlike Stephanovich *et al.* [14]. There is no doubt that for a realistic comparison with experiments these conditions should be taken into account. But this paper is devoted mainly to conceptual problems which, as we have already mentioned, prove to be fairly difficult by themselves. That is why we prefer not to divert the reader's attention from these conceptual problems. The only parameter which we shall try to calculate in this paper is the phase transition temperature for different total thicknesses of the pair of the layers, i.e., for various "periods" of the superstructure. We shall also analyze the form of the polarization profile setting in at the phase transition.

The paper is organized as follows: In Section 2 we deal with systems consisting of two or three layers of the ferroelectric and paraelectric materials ("small systems"). We begin this part with describing the ChT results relevant to what is considered in this paper. Also, we apply their approach to other three or two layer systems as a preparation to what will be considered in the next section. In Sec.3, we try to understand what happens in large systems considering first doubled "small systems" and then generalizing some of the results to systems of arbitrary length. The physical conclusions which can be made, to different degree of certainty, from the obtained results are discussed in Section 4. In Section 5 we shortly summarize the results of our paper.

II. SMALL SYSTEMS

A. The Chensky and Tarasenko approach

The system they studied is illustrated in Figure 1. The ferroelectric phase transition in this system may be either to single or multidomain states. Naturally, when the thickness of the paraelectric ("dead") layers is sufficiently small the transition will be into single domain state. ChT found the maximum dead layer thickness (d_c) for this phase transition. They

studied in detail only the case where the dead layer thickness is much smaller than the film thickness. For this case d_c proved to be independent of the ferroelectric slab thickness but depended on ferroelectric material constants and the dielectric constant of the paraelectric [16]. We are interested in the case where the two thicknesses are comparable, moreover, as we have mentioned we shall put them equal. Nevertheless, some general formulas of ChT are relevant to our case also and the phenomena in the cases of thin and thick dead layers for similar systems prove to be qualitatively similar. That is why it makes sense to expose some of ChT results and to describe their procedure to some detail.

Note that, first of all, for $d > d_c$ when the phase transition is into a multidomain state they found two types of the appearing domain structure. If $d - d_c < d_c$ the period of the domain structure was larger than the thickness of the ferroelectric slab ("wide domains",WD), for $d - d_c > d_c$ this period is less than the thickness ("narrow domains", ND). In Ref. 14 these two regimes were called "strong coupling" and "weak coupling" regimes. In this work, we shall see that in the case of sufficiently large dielectric constant of the paraelectric one has to distinguish between two different ND regimes.

To find the phase transition temperature, ChT studied stability of the paraelectric phase. The mathematical signal of a loss of stability of a state (phase) was obtained by studying solutions of an appropriate system of linear differential equations together with relevant boundary conditions. This method goes back to a paper by Suhl [17] who used it in another problem. The phase is stable when the only possible solution is zero (trivial). Appearance of non-zero (non-trivial) solutions signals a way of loss of stability of the phase and specifically this loss is with respect to a form of the ferroelectric polarization distribution which is represented by the solution. Within this formulation of the problem there is infinite number of ways of the stability loss represented by infinite set of the polarization distributions. Of course, they are not real, they are virtual possibilities of the stability loss. The real loss of stability of the paraelectric phase occurs with respect to a single form chosen among this infinite number of virtual solutions. The criterion of the choice is that the loss of stability of the paraelectric phase with respect to this solution occurs the earliest, i. e., it corresponds to the highest temperature.

Together with ChT we shall suppose that both the ferroelectric and paraelectric materials are isotropic in the $x - y$ plane. Then the nontrivial inhomogeneous solutions appear simultaneously for the inhomogeneities along all the directions in this plane. That is why

it is sufficient to consider inhomogeneities along one direction only which we identify with the x axis.The above mentioned system includes the linearized constituent equation for the ferroelectric polarization (P_z)

$$AP_z - g\frac{\partial^2 P_z}{\partial x^2} - \eta\frac{\partial^2 P_z}{\partial z^2} = E_z, \tag{1}$$

where E_z is the electric field along z and the y-derivative is omitted because of the reasons explained below. Also other equations should be included to take account for an (indirect) influence of P_z on other degrees of freedom. The most important of them is the polarization along x (nonferroelectric) axis. Since $E_z(x)$ implies the presence of E_x via the electrostatic equation $curl\mathbf{E} = 0$ one has to take into account this field together with the polarization which we shall implicitly take into account introducing the dielectric constant $\varepsilon_\perp$ along the plane of the structure. The electric field due to the ferroelectric polarization exists, of course, also in the paraelectric which we consider as isotropic with the dielectric constant ε_p. The system of equations become complete by adding $\operatorname{div}\mathbf{D} = 0$, where $\mathbf{D} = \varepsilon_0\varepsilon_p\mathbf{E}$ in the paraelectric and $\mathbf{D} = (\varepsilon_0\varepsilon_\perp E_x, 0, \varepsilon_0\epsilon_b E_z + P_z)$ in the ferroelectric one. In the latter formula we have introduced the so-called "base" dielectric constant, ϵ_b, which is the assumed to reflect the fact that P_z is not the the total z-component of the polarization but is only the "soft part" of the total polarization corresponding to the order parameter [18]. In this way we take into account more non-ferroelectric degrees of freedom.

Since we are considering an infinite slab we can present the x-dependence of all the functions in form of a Fourier series, e.g. $P_z(x,z) = \sum P_{zk}(z)\cos kx$ to see that the system of the partial differential equations decomposes into ordinary differential equations.It is convenient to use instead of electric field the electrical potential $\varphi(x,z)$. In addition, following ChT, we put $\eta = 0$ in Eq. 1 that considerably simplifies the mathematics and makes it possible to take into account the electrostatic boundary conditions only, which we have already commented in Section 1. Inserting the Fourier form of the polarization and the electrostatic potential, Eq. 1 converts into an algebraic equation:

$$\left(A + gk^2\right)P_{zk} = -\frac{d\varphi_k}{dz} \tag{2}$$

and for a given k the electrostatic equation $\operatorname{div}\mathbf{D} = 0$ acquires now the form

$$\varepsilon_k\frac{d^2\varphi_{fk}}{dz^2} - \varepsilon_\perp k^2\varphi_{fk} = 0, \tag{3}$$

where

$$\varepsilon_k = \epsilon_b + 1/\varepsilon_0 \left(A + gk^2\right) \tag{4}$$

for the ferroelectric. For the paraelectric layer we have

$$\frac{d^2\varphi_{pk}}{dz^2} - k^2\varphi_{pk} = 0 \tag{5}$$

Because of the symmetry of the system we establish that there are two families of the solutions: symmetric and antisymmetric with respect to reflection in the mirror plane at $z = 0$. ChT considered antisymmetric solutions only guided by physical arguments. We shall consider both families of solutions to illustrate our treatment of larger systems where these two solutions can, in principle, compete. In both cases one can use the boundary conditions at two of the four interfaces, e.g. at $z = l/2$ and $z = (l + d)/2$:

$$\varphi_k \left((l + d)/2\right) = 0 \tag{6}$$

$$\varphi_k \left(l/2 + 0\right) = \varphi_k \left(l/2 - 0\right) \tag{7}$$

$$\varepsilon_k \frac{d\varphi_k}{dz} \left(l/2 - 0\right) = \varepsilon_p \frac{d\varphi_k}{dz} \left(l/2 + 0\right) \tag{8}$$

One can show that for $\varepsilon_k > 0$ no nontrivial solution of either family is possible, i.e. the nonpolar phase is stable. For $\varepsilon_k < 0$ we begin with antisymmetrical case looking for solutions in the form $\varphi_{fk}(z) = C \sin qz$, where

$$q = k\sqrt{\varepsilon_\perp / \mid \varepsilon_k \mid} \tag{9}$$

for the ferroelectric and $\varphi_{pk}(z) = F \sinh k\left(z - (l + d)/2\right)$ for the paraelectric. Eqs. 7-8 attain the form

$$C \sin ql/2 + F \sinh kd/2 = 0 \tag{10a}$$

$$C\varepsilon_k q \cos ql/2 - F\varepsilon_p k \cosh kd/2 = 0 \tag{10b}$$

Non-trivial solutions for Eqs. 10a-b exist if

$$\tan ql/2 = \left(\sqrt{\mid \varepsilon_k \mid \varepsilon_\perp}/\varepsilon_p\right) \tanh kd/2 \tag{11}$$

In the limit of $d \to \infty$ this formula converts to

$$\tan ql/2 = \sqrt{\mid \varepsilon_k \mid \varepsilon_\perp}/\varepsilon_p \tag{12}$$

which is relevant to phase transition to multidomain state in a non-electroded plate in an infinite medium with the dielectric constant ε_p. We shall repeatedly revisit this formula throughout this paper.

For the symmetrical case instead of Eq. 11 we start from $\varphi_{fk}(z) = C\cos qz$. Then instead of Eqs. 10a-b, we have

$$C\cos ql/2 + F\sinh kd/2 = 0 \tag{13a}$$

$$C\varepsilon_k q\sin ql/2 + F\varepsilon_p k\cosh kd/2 = 0 \tag{13b}$$

from where the condition of nontrivial solution is obtained as

$$\tan ql/2 = -\left(\varepsilon_p k/\sqrt{\mid \varepsilon_k \mid \varepsilon_\perp}\right)\coth kd/2 \tag{14}$$

Since the negative sign of the r.h.s. of this equation the argument of the tangent should be more than $\pi/2$ unlike to Eq.11, it should be noted that for the same value of k the value of q for the symmetric family is larger than that for the antisymmetric, i.e. $\mid \varepsilon_k \mid$ is less in the symmetric case than in the antisymmetric. From Eq. 4 one sees that this corresponds to larger $\mid A \mid$, i.e., to a lower temperature of the stability loss than for the solution with the same k from the antisymmetric family. Physically, this is quite natural: a symmetric potential in the ferroelectric layer mean that both the electric field and the ferroelectric polarization (See Eq. 4) are zero at the central plane of the slab that is energetically less profitable than to have the polarization of the same sign for all the values of z. Therefore, one has to discuss Eq.11 only to find the function $A_{ls}(k)$ which defines the limit of stability of the nonpolar phase with respect to the appearance of "polarization wave" with a given k. As we have already mentioned, to find the real limit of the stability one has to find the "weakest point", i.e. the value of k which corresponds to the maximum value of $A_{ls}(k)$ where the "first" stability loss with the highest temperature occurs.

B. The Chensky-Tarasenko cell with thick deadlayer

It is easy to find function $A_{ls}(k)$ for small k and large k regions. ChT found it for the case of very thin dead layer but it is straightforward not make this assumption and the cell considered in this section is displayed in Figure 2. To avoid overloading of the paper by

formulas we shall not consider the general case but only that of $d = l$, i.e. we have:

$$\tan ql/2 = \left(\sqrt{\mid \varepsilon_k \mid \varepsilon_\perp}/\varepsilon_p\right) \tanh kl/2 \tag{15}$$

For small k region one can expand the both sides of Eq. 15 in terms of k and q taking first into account two first terms only.

$$\sqrt{\frac{1}{\mid \varepsilon_k \mid_{ls}}} \left(1 + \frac{\varepsilon_\perp k^2 l^2}{12 \mid \varepsilon_k \mid_{ls}}\right) = \frac{\sqrt{\mid \varepsilon_k \mid_{ls}}}{\varepsilon_p} \left(1 - \frac{k^2 l^2}{12}\right) \tag{16}$$

Putting in this equation $k = 0$ and also differentiating it with respect to k^2 and then putting $k = 0$ we find two first terms in the Taylor expansion for $\mid \varepsilon_k \mid_{ls}$ in terms of k^2.

$$\mid \varepsilon_k \mid_{ls} = \varepsilon_p + \frac{k^2 l^2 \left(\varepsilon_p + \varepsilon_\perp\right)}{12} \tag{17}$$

Using Eq. 4 one obtains

$$A_{ls} = -\frac{1}{\varepsilon_0 \left(\varepsilon_b + \varepsilon_p\right)} + \left(\frac{l^2 \left(\varepsilon_p + \varepsilon_\perp\right)}{12\varepsilon_0 \left(\varepsilon_b + \varepsilon_p\right)^2} - g\right) k^2 + ... \tag{18}$$

The first term corresponds to the loss of stability with respect to a single domain state. Depending on the sign of the coefficient at k^2 the loss of stability with respect to a "polarization wave" with $k \neq 0$ coresponds to larger or smaller values of A, i. e. to an "earlier" or to a "later" event. Since the "later" stability loss is of no interest, the phase transition is into a multidomain state if the coefficient is positive and is, probably, to a single domain state if the coefficient is negative. The word "probably" takes into account an a-priori possibility that at larger values of k the function $A_{ls}(k)$ grows and acquires values larger that the first term. We shall show below that this possibility is not realized for sufficiently small l, i.e. the single domain or the small-k (wide domain - WD) regimes are possible for small l only. Zero value of the coefficient at k^2 in Eq. 18 defines the "critical" value of l (l_c) which separates the phase transitions into single and multi-domain states. For $l < l_c$ the function $A_{ls}(k)$ has maximum at $k = 0$. One can thus see that

$$l_c^2 = 12\varepsilon_0 g \left(\varepsilon_b + \varepsilon_p\right)^2 / \left(\varepsilon_p + \varepsilon_\perp\right) \simeq .12\varepsilon_0 g \varepsilon_p^2 / \left(\varepsilon_p + \varepsilon_\perp\right), \tag{19}$$

where we have supposed that $\varepsilon_p \gg \varepsilon_b$ that is usually the case for systems of experimental interest. We shall restrict ourselves by this case only. It follows from Eq. 19 that since

$\varepsilon_0 g \simeq 1\,\text{Å}^2$ (See, e. g. Ref.19) one finds for $\varepsilon_\perp \gg \varepsilon_p$ that l_c is less than unit cell distance, i.e. no phase transition into single domain state is possible. If, on the contrary, $\varepsilon_p > \varepsilon_\perp$ which is what one has for $BaTiO_3$-$SrTiO_3$ superstructure, the l_c can be considerably larger than the unit cell distance and our use of a continuous medium theory to consider interplay between single- and multidomain formation at the phase transition is quite consistent and valid. We shall keep our focus on this case.

We begin with the small k (WD) region by finding the next, k^4, term in Eq. 18. One has to take into account the next terms in expansions of the tan and tanh in Eq. 15 to obtain :

$$\sqrt{\frac{1}{\mid \varepsilon_k \mid_{ls}}}\left(1+\frac{\varepsilon_\perp k^2 l^2}{12 \mid \varepsilon_k \mid_{ls}}+\frac{\varepsilon_\perp^2 k^4 l^4}{120 \mid \varepsilon_k \mid_{ls}^2}\right)=\frac{\sqrt{\mid \varepsilon_k \mid_{ls}}}{\varepsilon_p}\left(1-\frac{k^2 l^2}{12}+\frac{k^4 l^4}{120}\right) \tag{20}$$

Differentiating this equation with respect to k^2 two times and putting then $k=0$ we find

$$\mid \varepsilon_k \mid_{ls} = \varepsilon_p + k^2 l^2 \left(\varepsilon_p + \varepsilon_\perp\right)/12 + k^4 l^4 \left(\varepsilon_\perp^2 - \varepsilon_p^2\right)/\left(720\varepsilon_p\right) \tag{21}$$

$$\varepsilon_0 A_{ls} = -\frac{1}{\varepsilon_p} + \frac{\left(l^2 - l_c^2\right)\left(\varepsilon_p + \varepsilon_\perp\right)}{12\varepsilon_p^2} k^2 - \frac{\left(\varepsilon_\perp + \varepsilon_p\right)\left(3\varepsilon_p + 2\varepsilon_\perp\right) k^4 l^4}{360\varepsilon_p^3} \tag{22}$$

For $l > l_c$ the value of k corresponding to the maximum of function $A_{ls}(k)$ and, therefore, to the phase transition is

$$k^2 = k_c^2 = \frac{15\left(l^2 - l_c^2\right)\left(\varepsilon_p + \varepsilon_\perp\right)}{l^4\left(3\varepsilon_p + 2\varepsilon_\perp\right)} \simeq \frac{5\left(l^2 - l_c^2\right)}{l^4}, \tag{23}$$

where once more we have assumed that $\varepsilon_p > \varepsilon_\perp$. We see from this formula that the WD regime ($kl < 1$) is possible only at, approximately,

$$l - l < l_c/3, \tag{24}$$

i. e., the range of l corresponding toWD is fairly small. The phase transition temperature is determined by

$$\varepsilon_0 A_{ls}\left(k_c\right) = -\frac{1}{\varepsilon_p}\left(1 - \frac{5\left(l - l_c\right)^2\left(\varepsilon_p + \varepsilon_\perp\right)}{2l_c^2\left(3\varepsilon_p + 2\varepsilon_\perp\right)}\right), \tag{25}$$

where Eq. 24 is taken into account. Before making sure that Eq. 25 is valid when condition Eq. 24 is fulfilled, we have to check if the condition related to the possibility to develop the tan,i.e. $q_c l < 1$, is satisfied. One sees from Eq. 25 that at the boundary of the WD regime, i.e. at $l - l_c \simeq l_c/3$ the value of $A_{ls}(k_c)$ is nearly the same as for $l = l_c$, i.e. $\mid \varepsilon_k \mid_{ls} \simeq \varepsilon_p$. Taking into account Eq. 9 we see that at the boundary of the WD regime is $q_c \mathrm{l} \simeq \sqrt{\varepsilon_\perp/\varepsilon_p}$.

This means that if $\varepsilon_p \gg \varepsilon_\perp$ there exists a narrow domain (ND) regime with small changes of the values (electric field, polarization) across the ferroelectric layer. We shall call it the NDS regime.

Since within this regime $q_c l < 1$ while $k_c l > 1$, Eq. 15 can be approximated as

$$ql/2 = \sqrt{\mid \varepsilon_k \mid \varepsilon_\perp}/\varepsilon_p \tag{26}$$

or

$$\mid \varepsilon_k \mid = \varepsilon_p kl/2. \tag{27}$$

Using then Eq. 4 one obtains

$$A_{ls}(k) = -2\left(\varepsilon_0 \varepsilon_p kl\right)^{-1} - gk^2 \tag{28}$$

The maximum of this function corresponds to

$$k = k_c = \left(\varepsilon_0 \varepsilon_p gl\right)^{-1/3} \tag{29}$$

and the expected phase transition temperature is defined by

$$A_{ls}(k_c) = -2\left(\varepsilon_0 \varepsilon_p gl\right)^{1/3}\left(\varepsilon_0 \varepsilon_p l\right)^{-1} - g\left(\varepsilon_0 \varepsilon_p gl\right)^{-2/3} = -3g^{1/3}\left(\varepsilon_0 \varepsilon_p\right)^{-2/3} l^{-2/3} \tag{30}$$

The NDS regime, which evidently begins at $l \simeq (1.5-2)\, l_c$, ends when $q_c l$ approaches unity. Using Eqs. 26, 27 and 29, one finds that it happens around

$$l \simeq l_\sim = \left(\varepsilon_p/\varepsilon_\perp\right)^{3/2} l_c \tag{31}$$

One sees that if $\varepsilon_p \gg \varepsilon_\perp$the NDS regime corresponds broad interval of l.

At $l > l_\sim$ one has $\tan ql/2 \gg 1$ (NDL regime with large change of values across the thickness of the layer) or

$$q \simeq \pi/l \tag{32}$$

i. e. it is the case well studied by ChT who showed (See also Ref. 19) that for the phase transition and the period of the sinusoidal domain structure one has:

$$A_{ls}(k_c) = -2\pi g^{1/2}\left(\varepsilon_0 \varepsilon_\perp\right)^{-1/2} l^{-1} \tag{33}$$

$$k_c^2 = \pi\left(\varepsilon_0 \varepsilon_\perp g\right)^{-1/2} l^{-1} \tag{34}$$

We see that here the phase transition point as well as the period of the domain structure does not depend on ε_p. The two last equation are valid also for ferroelectric phase transition in a non-electroded plate that is quite natural because together with the film thickness, the thickness of the two paraelectric "dead layers" become very large. We illsutrate the results in Figure 3 using Eq. 22 for the small l regime and Eq. 30 for the large l regime in comparison with the numerical solution of Eq. 15 for a maximum l of 20 nm .

C. Bilayer

Figure 4 illustrates the system we want to discuss now. It is straightforward within the ChT approach exposed in the previous Subsection. The solutions for $\varphi_k(z)$ are now $\varphi_k(z) = C \sin qz$ for the ferroelectric layer and $\varphi_k(z) = F \sinh k(z - 2l)$ for the paraelectric one. The boundary conditions at $z = l$ are:

$$C \sin ql + F \sinh kl = 0 \tag{35}$$

$$C\varepsilon_k q \cos ql - F\varepsilon_p k \cosh kl = 0 \tag{36}$$

Comparing with Eqs.10a-b for $d = l$ we see that one has to substitute l for $2l$ in this equation to obtain Eqs. 35-36 so that instead of Eq. 15 one has:

$$\tan ql = \left(\sqrt{\mid \varepsilon_k \mid \varepsilon_\perp}/\varepsilon_p\right) \tanh kl \tag{37}$$

In the same way all the results from the previous Subsection can be converted into the results for the bilayer. In particular, one sees that the critical value of l separating the single domain and the wide domain regimes is now 2 times less than in the previous case. Also, for very large l's the difference between the phase transition temperature and the Curie temperature T_c ($A(T_c) = 0$) is 2 times smaller in the case of the bilayer than in the ChT case of a symmetrical trilayer. The transition temperatures and k_c as a function of layer thickness for three different values of ε_p are given in Figure 5.

D. Non-symmetrical trilayer

Before any algebra, one can expect the critical value of l to be larger than for the bilayer and smaller than for the simmetrical trilayer. For very large l's one expects that the limit

will once more correspond to isolated ferroelectric layer, i.e. Eqs. 26-27 will be valid for very large l's in this case also. The situation with a more interesting intermediate l's case described by Eqs. 33-34 is less clear and this motivates us to consider this case explicitely.

The system and the notations are presented in Figure 6. We write the solutions for the potential in the form:

$$\varphi_k(z) = F_1 \sinh kz \tag{38}$$

for $0 < z < l_1$

$$\varphi_k(z) = C \sin q(z - l_1) + D \cos q(z - l_1) \tag{39}$$

for $l_1 < z < l_1 + l$ and

$$\varphi_k(z) = F_2 \sinh k(z - 2l) \tag{40}$$

for $l_1 + l < z < 2l$. The boundary conditions at $z = l_1$ read:

$$C \sinh kl_1 = D \tag{41}$$

$$\varepsilon_p k F_1 \cosh kl_1 = - \mid \varepsilon_k \mid qC \tag{42}$$

and at $z = l_1 + l$:

$$C \sin ql + D \cos ql = -F_2 \sinh k(l - l_1) \tag{43}$$

$$- \mid \varepsilon_k \mid q(C \cos ql - D \sin ql) = \varepsilon_p k F_2 \cosh k(l - l_1). \tag{44}$$

With the help of Eqs. 41, 42 it is easy to reduce the system to two equations only:

$$F_1(\mid \varepsilon_k \mid q \sinh kl_1 \cos ql - \varepsilon_p k \cosh kl_1 \sin ql) + F_2 \mid \varepsilon_k \mid q \sinh k(l - l_1) = 0 \tag{45}$$

$$C_1(\varepsilon_p k \cosh kl_1 \cos ql + \mid \varepsilon_k \mid q \sinh kl_1 \sin ql) - F_2 \varepsilon_p k \cosh k(l - l_1) = 0. \tag{46}$$

The condition of existence of non-trivial solutions of this system reads

$$\left[(\varepsilon_p k)^2 - \mid \varepsilon_k \mid^2 q^2 \tanh kl_1 \tanh k(l - l_1)\right] \tan ql = \mid \varepsilon_k \mid qk\varepsilon_p \left[\tanh k(l - l_1) + \tanh kl_1\right]. \tag{47}$$

To be specific we shall assume that $l_1 < l/2$, i.e. $l - l_1 > l/2$. For large l's we expect that $kl_1 \gg 1$ then also $k(l - l_1) \gg 1$. In this case the both tanh $\simeq 1$ and Eq. 47 acquires the form

$$\tan ql = \frac{2 \mid \varepsilon_k \mid qk\varepsilon_p}{(\varepsilon_p k)^2 - a^2 q^2}$$

or

$$\tan ql/2 = \frac{\mid \varepsilon_k \mid q}{\varepsilon_p k} = \frac{\sqrt{\mid \varepsilon_k \mid \varepsilon_\perp}}{\varepsilon_p},$$

that coincides with Eq. 12.

We see that for sufficiently large l's the system "forgets" the absence of symmetry. However, for small l the situation is different. Let us find l_c for this case. To realize this aim, one has to expand tanh's and tan in Eq. 47 keeping two first terms only. As a result one finds that

$$\mid \varepsilon_k \mid = \varepsilon_p \left(1 + \frac{(\varepsilon_\perp + \varepsilon_p) k^2}{3\varepsilon_p} \left(l^2 - 3l_1 (l - l_1)\right)\right) \tag{48}$$

$$A_{ls}(k) = -\frac{1}{\varepsilon_0 (\varepsilon_b + \varepsilon_p)} + \left(\frac{(\varepsilon_\perp + \varepsilon_p)}{3\varepsilon_0 (\varepsilon_b + \varepsilon_p)^2} l^2 \left(1 - 3\frac{l_1 (l - l_1)}{l^2}\right) - g\right) k^2, \tag{49}$$

i. e., in this case

$$l_c^2 = \frac{3g\varepsilon_0 (\varepsilon_b + \varepsilon_p)^2}{(\varepsilon_\perp + \varepsilon_p)\left(1 - 3\frac{l_1(l-l_1)}{l^2}\right)}. \tag{50}$$

We see that at $l_1 = l/2$ Eq. 50 coincides with Eq. 19. while at $l_1 = 0$ it provides l_c which is 1/2 of the previous one. Figure 7 illustrates the dependences of the phase transition temperature and of q_c, k_c on l for all the cases (ChT cell, bilayer cell and non-symmetrical trilayer) considered above. Note that in all three cases, the transition temperature into the single domain state is the same.

III. LARGE SYSTEMS

We want now to discuss a systems with many layers. There is a temptation to consider it as infinite, i. e. to consider a repeating unit ("unit cell") and apply periodic boundary conditions at the boundaries of the unit. Implicitely by doing this one assumes that the conditions at the boundaries of the multilayer structure are negligible. This was the way in which the authors of Refs.14 and 15 modeled the superlattice systems. Here, we start with the boundary conditions at the oxide-electrode interfaces for different repeating cells (ChT or bilayer and etc.) of the superstructure and demonstrate that these systems are very sensitive both to electrostatic boundary conditions as well as the layer sequence. The schematics of the two systems are given in Figure 8.

In fact, the assumption about periodicity, i. e., irrelevance of conditions at the boundaries of a very large multilayer structure, can be questioned from simple physical arguments. Let

us consider the virtual loss of stability of the paraelectric phase in a very large multilayer structure with respect to a single domain ferroelectric state assuming the periodicity along the thickness of the structure. Assuming periodic boundary condititons is equivalent to consider the unit cell as a small system with short circuited electrodes. We have found out that in the previous Section, the loss of stability of the paraelectric state to single domain ferroelectric state occurs at

$$A_{ls}\left(0\right)=-\varepsilon_{0}^{-1}\left(\varepsilon_{b}+\varepsilon_{p}\right)^{-1} \tag{51}$$

(Compare with Eqs. 18, 49). Let us show that this result is not necessarily correct. Whether Eq. 51 is correct or not depends on if the multilayer system as whole is supplied by metallic electrodes and these electrodes are short-circuited. Imagine that there are no such electrodes. Then from the conditions $dD_z/dz = 0$ inside the superstructure and that $\mathbf{D} = 0$ beyond the multilayer gives us the result that $\mathbf{D} = 0$ at every point of the multilayer (recall that we consider a possible single domain state, i. e. there is no dependencies along the x and y axes). As a result for a homogeneously polarized state

$$E_{z}=-P_{z}/\left(\varepsilon_{b}\varepsilon_{0}\right), \tag{52}$$

and from Eq. 1 it follows that

$$\left(A+\varepsilon_{0}^{-1}\varepsilon_{b}^{-1}\right)P_{z}=0, \tag{53}$$

i. e. the loss of stabilty of the paraelectric phase with respect to a single domain state occurs at

$$A_{ls}=-\varepsilon_{0}^{-1}\varepsilon_{b}^{-1} \tag{54}$$

that differs very substantially from Eq. 49. In other words, the loss of stability of the paraelectric phase with respect to appearance of a single domain ferrolectric state depends on the conditions at the boundaries of the multilayer, i. e. the idea about an infinite multilayer cannot be applied to this problem. Physically, this is quite natural because both in this work and work of others [14,15] one considers layers of infinite lateral sizes, i. e., the sizes of the external electrodes or of a non-electroded external surface is always larger that full thickness of the multilayer system. Experimentally, the ratio of the lateral sizes and the thickness is never less than at least an order of magnitude. Therefore, no point inside the multilayer system is "far enough" from the surface. We argue in Section 4 that the case of complete absence of electrodes or any short circuiting is of fairly academic nature

and the periodic boundary conditions are acceptable almost irrespective of these conditions. However, it is not necessarily so for the phase transition into multidomain states.

To understand where the latter statement comes from let us consider a system of two bilayers (Figure 9). One sees that the conditions for screening of the stray electric field arizing beyond a ferroelectric layer when a domain structure is formed in the layer are different for the layer 1 and the layer 2. In the first layer a stray field beyond the ferroelectric exists on one side only while in the second layer it exists on the two sides. Thus, it is evident that the polarization profile at the phase transition will be different in the two ferroelectric layers. It is worthwhile to consider this case in more detail since the number of the ferroelectric-paraelectric interfaces is still relatively small and the treatment of this case can be performed without too much algebra.

A. Two bilayers

The solutions for $\varphi_k(z)$ we shall write in the form $\varphi_{f1k}(z) = C_1 \sin qz$ and $\varphi_{f2k}(z) = C_2 \sin q(z-2l) + D_2 \cos q(z-2l)$ for the two ferroelectric layers and $\varphi_{p1k}(z) = F_1 \sin q(z-l) + G_1 \cos q(z-l)$ and $\varphi_{p2k}(z) = F_2 \sin q(z-4l)$ for the two paraelectric layers. The short-circuited electrodes are taken into account in the first and in the last formulas.

It is convenient to introduce here dimensionless parameters:

$$\alpha = \mid \varepsilon_k \mid /\varepsilon_p, \xi = \varepsilon_p/\varepsilon_\perp \tag{55}$$

Note that to the loss of stability with respect to homogeneous polarization corresponds to $\alpha = 1$ and the values of α of interest are larger than unity.

From the boundary conditions at $z = l$ one finds

$$G_1 = C_1 \sin ql, \quad F_1 = -C_1\sqrt{\alpha/\xi}\cos ql. \tag{56}$$

Next, from the boundary conditions at $z = 2l$ we find

$$C_2 = C_1\left(\cos ql \cosh kl - \sqrt{\xi/\alpha}\sin ql \sinh kl\right), \quad D_2 = C_1\left(-\sqrt{\alpha/\xi}\cos ql \sinh kl + \sin ql \cosh kl\right) \tag{57}$$

and from the conditions at $z = 3l$ two formulas for F_2 are

$$F_2 = C_1\left[\sqrt{\xi/\alpha}\sin^2 ql + \sqrt{\alpha/\xi}\cos^2 ql - \sin 2ql \coth kl\right] \tag{58}$$

and

$$F_2 = C_1 \left[2^{-1} \sin 2ql \tanh kl \, (1 - \alpha/\xi) - \sqrt{\alpha/\xi} \cos 2ql \right] \tag{59}$$

The equivalence of these formulas gives us the condition of the existence of non-trivial solutions which can be written as a quadratic equation for $\tan ql$

$$\left(\sqrt{\xi/\alpha} - \sqrt{\alpha/\xi} \right) \tan^2 ql - [(1 - \alpha/\xi) \tanh kl + 2 \coth kl] \tan ql + 2\sqrt{\alpha/\xi} = 0, \tag{60}$$

whose solutions are

$$(\tan ql)_1 = \sqrt{\alpha/\xi} \tanh kl \tag{61a}$$

$$(\tan ql)_2 = \frac{2 \coth kl}{\sqrt{\xi/\alpha} - \sqrt{\alpha/\xi}} \tag{61b}$$

Note that Eq. 61a coincides with Eq. 37 for a bilayer but before concluding that the phase transition temperature in the two-bilayer is the same as in a single-bilayer, one has to study the possible stability losses which follow from Eq. 61b to figure out if these stability losses correspond to lower temperatures than those following from Eq. 61a. At $\xi \gg 1$ there is an interval of values of $\alpha : 1 < \alpha < \xi$ which is both of interest ($\alpha > 1$) and correspond to the positive sign of the l.h.s. of Eq. 61b. Since $q = k\sqrt{1/\alpha\xi} < k$ the solutions of Eq. 61b are possible for $kl > 1$ and $\coth kl$ can be replaced by unity. Eq. 61b then reads

$$ql = 2\sqrt{\alpha/\xi} \tag{62}$$

that coincides with Eq. 26 discussed before. We have seen there that it is related to loss of stability of the paraelectric phase in ChT cell which occurs at lower temperatures than in the bilayer system. This means that the solution given by Eq. 61b is irrelevant to our studies. We shall discuss the physical reason of this irrelevance in the upcoming sections where we explain in detail why we think 61b indeed corresponds to a "later" loss of stability compared to 61a.

It is worthwhile to discuss the profile of the polarization arizing at the phase transition. From Eqs. 57 and 61a one sees that $D_2 = 0$ and

$$C_2 = C_1 \cos ql / \cosh kl, \tag{63}$$

i. e. the polarization in the first and second ferroelectric layer is

$$P_{zf1} = C_1 \mid \varepsilon_k \mid \cos qz \cos kx \tag{64a}$$

$$P_{zf2} = \frac{C_1 q \cos ql}{\cosh kl} \mid \varepsilon_k \mid \cos q\,(z - 2l) \cos kx \tag{64b}$$

that is the amplitude of the "polarization wave" is smaller in the second ferroelectric layer as than is the first one (Eq. 38) as we have expected from the begining and becomes exponentially small in the narrow domain regime. For the paraelectric layers we have

$$\varphi_{p1} = -\frac{C_1 \sin ql}{\sinh kl} \sinh k\,(z - 2l) \tag{65a}$$

$$\varphi_{p2} = -C_1 \frac{\cos ql \sin ql}{\cosh ql \sinh kl} \sinh k\,(z - 4l) \tag{65b}$$

Note that despite there is no electrode at $z = 2l$, i.e. between the first paraelectric and the second ferroelectric layer the potential is zero at this interface.

Now we want to see the polarization profile, which corresponds to the second option given by Eq. 61b. We shall compare the amplitude of the "polarization wave" in the two ferroelectric layers. We should use to this end Eq. 57 together with Eq.61b. For the same conditions of the parameters which are necessary for existence of solution of Eq. 61b ($\alpha < \xi$, $kl > 1$) we find for the polarization in the second ferroelectric layer

$$P_{zf2} = -C_1 q \cos ql \cosh kl \mid \varepsilon_k \mid \cos \left[q\,(z - 2l) - 2\,(\alpha/\xi)^{3/2} \right] \tag{66}$$

We see that for this option the ferroelectric polarization in the second layer is larger than in the first one (it is also in opposite direction). So it is quite natural that this latter option is less profitable for the system and corresponds to a loss of stability at a lower temperature.

B. Many bilayers

It is already for a three-bilayer system that the calculations become inconvenient. Instead of Eq. 60 one obtains a third-order equation for $\tan ql$ with coefficients given by awkward formulas. Though one of the three solutions is still given by Eq. 61a, to analyze the stability loss corresponding to two other possible families (in the case that the third order equation has three real roots) seems to be beyond the present work. Considering more bilayers is even more prohibitive. What we can easily show is that Eq. 61a is relevant to any number of bilayers. It is tempting to conclude from this fact that the phase transition temperature is the same for a short-circuited multilayer system consisting of any number of bilayers. This seems physically reasonable but, unfortunately, we cannot show this mathematically because

to do so we are obliged to study loss of stability with respect to solutions corresponding to all the families of solutions and the number of the families seem to increase concurrent with the number of the ferroelectric layers in the system. We have seen for the case of the two-bilayer system that the second family cannot compete with the first one corresponding to Eq. 61a. But we see no easy way to show this for any number of the bilayers when the number of the families could be equal or at least comparable with the number of the bilayers. Thus we can only propose physical arguments to elaborate on the earliest loss of stability. One must note that the phase transition temperature in a single bilayer system is higher than in what we called the ChT cell with the same total thickness of the ferroelectric and the paraelectric because the ferroelectric in the bilayer system is in a "better position" for forming a multidomain system than in the ChT one: A part of the stray field associated with the domains is absent due to the electrode, i. e., the energy cost of formation of the domain structure is less in this ferroelectric layer than in the ferroelectric layer in the ChT system. This priviledge of the first ferroelectric layer which is in contact with the electrode is conserved in a system with any number of the bilayers. Therefore, it is quite natural that the profile of the polarization amplitude of the "polarization wave" appearing at the phase transition is larger in the first layer than in other layers which have no direct contact with an electrode. This is just what is given by the solution of Eq. 61a that we have seen for the case of a two-bilayer system. This is because we think that other solution options which arise are similar to the one given by Eq. 61b are irrelevant to the transition, also supported by the results of our numerical simulations as discussed in the forthcoming section.

Technically, to show that the option given by Eq. 61a exists, we first guess and iterate on the form of the solutions which correspond to this option for a system with any number of bilayers and then we show that for this form the boundary conditions are satisfied if Eq. 61a holds. To guess the form we have considered three- and four-bilayer systems assuming from the beginning validity of Eq. 61a. The problem simplifies drastically and since we were able to satisfy the boundary conditions our initial assumption proves to be valid. As a result we have guessed that the solution is of the form

$$\varphi_{fn} = C_1 \frac{\cos^{n-1} ql}{\cosh^{n-1} kl} \sin q\left(z - 2\left(n-1\right) l\right) \tag{67}$$

for n-th ferroelectric layer and

$$\varphi_{pn} = -C_1 \frac{\cos^{n-1} ql \sin ql}{\cosh^{n-1} kl \sinh kl} \sinh k\left(z - 2nl\right) \tag{68}$$

for n-th paraelectric layer.

Now we have to check if Eq. 61a makes it possible to satsify the boundary conditions at the two interfaces of the $n-$th ferroelectric layer. To check the boundary conditions between the $(n-1)$-th paraelectric layer layer and the n-th ferroelectric layer ($z = 2(n-1)l$) we mention first that

$$\varphi_{pn-1} = -C_1 \frac{\cos^{n-2} ql \sin ql}{\cosh^{n-2} kl \sinh kl} \sinh k\left(z - 2(n-1)l\right) \tag{69}$$

Comparing Eq. 67 and 68 we see that the continuity of the potential is satisfied. The condition of continuity of the normal component of the dielectric displacement reads

$$\varepsilon_p k C_1 \frac{\sin ql}{\sinh kl} = aqC_1 \frac{\cos ql}{\cosh kl} \tag{70}$$

and is satified if Eq. 61a holds.

At the interface between the n-ferroelectric layer and the n-th paraelectric layer ($z = (2n-1)l$) the potential is non-zero but it is the same at the ferroelectric and at the paraelectric sides. The condition of continuity of the normal component of the dielectric displacement reads now

$$aqC_1 \cos ql = \varepsilon_p k C_1 \frac{\sin ql}{\sinh kl} \cosh kl \tag{71}$$

and it is once more satisfied if Eq. 61a holds. Therefore, we have proved that Eq. 61a provides condition of existence of non-trivial solutions given by Eqs. 67 and 68 for a system consisting of any number of the bilayers. Figure 10 presents dependence of the amplitude of the "polarization wave" in ferroelectric and paraelectric layers appearing at the loss of stability of the paraelectric phase computed using Eqs. 67 and 68.

C. Two Chensky-Tarasenko cells

The system we consider in this Subsection is presented in Figure 11. We can use its symmetry with respect to the mirror plane at the middle of the central paraelectric layer to find the possible solutions. Apart from antisymmetric solutions of potential which correspond to identical polarization profiles in the two ChT cells, it is possible to have symmetric solutions. It is evident that the condition of existence of antisymmetric solutions is given by Eq. 15. Let us now find the condition for existence of symmetrical solutions. For the central paraelectric layer such a solution can be only of type $\varphi_{p2} = G_2 \cosh kz$ and for the

third layer it is $\varphi_{p3} = F_3 \sinh k\,(z - 2l)$ and for the second ferroelectric layer we shall take it in a general form $\varphi_{f2} = C_2 \sin qz + D_2 \cos qz$ while for the first ferroelectric layer it is to be found using the symmetry. From the boundary conditions at $z = l/2$ one finds that

$$C_2 = G_2 \left(\sin ql/2 \cosh kl/2 - \sqrt{\xi/\alpha} \sinh kl/2 \cos ql/2 \right) \tag{72}$$

and

$$D_2 = G_2 \left(\cos ql/2 \cosh kl/2 + \sqrt{\xi/\alpha} \sin ql/2 \sinh kl/2 \right). \tag{73}$$

>From the boundary conditions at $z = 3l/2$ we find

$$C_2 = -G_3 \left(\sin q3l/2 \sinh kl/2 + \sqrt{\xi/\alpha} \cosh kl/2 \cos q3l/2 \right) \tag{74}$$

and

$$D_2 = -G_3 \left(\cos q3l/2 \sinh kl/2 - \sqrt{\xi/\alpha} \sin q3l/2 \cosh kl/2 \right) \tag{75}$$

Equating then two formulas for C_2 and D_2 we obtain a system of two equations for G_2 and G_3 and find the condition of existence of non-trivial solutions of this system. The latter proves to be given by Eq. 61b which we have already discussed considering two bilayers.

Now the importance of this family of solutions is quite different, however. For large ξ there is an interval of l where the two families of the solutions appear practically at the same temperature (See Figure 12) Recall that a symmetrical solution means that the vectors of the ferroelectric polarizations are of opposite directions in the two ferroelectric layers. In a real, not exactly equlibrium situation, loss of stability may occur with respect to solutions of the two families, i. e. the profile of the polarization arising at the phase transition may correspond to any linear combination of these solutions. Physically this is quite natural and correspond to that at large values of l the domain structures form practically independently in the two ferroelectric layers.

D. Many Chensky-Tarasenko cells

The same method as we applied to many bilayers can also be applied to a multilayer consisting of integer number of ChT cells whose schematic is already given in Figure 8b. Here, there are no "privileged" ferroelectric layers and it is natural to expect that the profile of the polarization will be the same in all the ferroelectric (paraelectric) layers. Starting from

Eqs. 10a-10b we can write down the expected solution for this case as

$$\varphi_{fnk} = C \sin q \left(z - \frac{4n-3}{2} l \right) \tag{76a}$$

$$\varphi_{pnk} = C \frac{\sin ql/2}{\sinh kl/2} \sinh k \left(z - \frac{4n-1}{2} l \right) \tag{76b}$$

One can easily check that the both boundary conditions are satisfied at both interfaces ($z = 2\,(n-1)\,l$ and $z = (2n-1)\,l$ of n-th ferroelectric layer if Eq. 15 holds. The polarization profile in the case of stability loss of the paraelectric phase to a multidomain polar state ($l = 5$ nm and 8 nm) is given in Figure 13.

IV. DISCUSSION

We have considered two types of superstructures consisting of either arbitrary number of bilayers or of what we called the ChT cells. The two superstructures are different only in nature of the layers in contact with the electrodes. In the bilayer case, there is immediate contact between a ferroelectric layer and the ideal metallic electode while the opposite electrode is in contact with a paraelectric layer. In the second case, both layers contacting the electrodes are paraelectric of the thickness $l/2$, where l is the thickness of both the paraelectric (total) and ferroelectric layers.We tried to calculate the ferroelectric phase transition temperature and to define the space distribution of ferroelectric polarization appearing at the phase transition when the electrodes are short-circuited. The method was to study the possible ways of stability loss of the nonpolar phase and to identify the one which occurs the first upon lowering the temperature. In this manner, one obtains both the phase transition temperature and the profile of the space distribution of the polarization just below the phase transition temperature.

The problem we attacked proved to be too difficult to be rigiorously solved because it became clear that in general in a large superstructure containing uniaxial ferroelectric layers with polar axis perpendicular to the layer plane, the ferroelectric polarization appearing at the phase transition is not periodic along the superstructure if the phase transition is into a multidomain state. This makes the number of different types of the polarization profiles with respect to which the nonpolar phase loses its stability to be comparable with the number of the unit cells in a given superstructure. We were able to perform an exhaustive analysis of

the loss of stability of the nonpolar phase only in two smallest "superstructures" consisting of two bilayers or two ChT cells. We found two types of the stability loss for every "small superstructure". A comparison of these solutions are in Figure 12. We have also shown that one of two types, specifically, those which correspond to the phase transitions in two-bilayer or in two-ChT cells systems are present in systems of any number of the bilayers or the ChT cells. We cannot prove mathematically that these types of the stability losses correspond to the phase transitions in very large superstructures as well but we find this feasible physically and we assume this as a hypothesis. Therefore, when we mention "phase transition" in a superstructure we mean, strictly speaking, a hypothetical phase transition which is also supported by our numerical simulations (See Figure 14).

We found that if the dielectric constant of the paraelectric layer, ε_p, is larger than than $\varepsilon_\perp$, then there is an interval of l's for which the ferroelectric phase tranition is into a single domain state. This interval goes from formally zero l (physically, of course, not less than unit cell distance) till some l which can be considerably larger than the unit cell size if ε_p is sufficiently large. We pay the main attention to this case where our continuous medium approach is well justified. The maximum l which corresponds to the single domain regime we call l_c. Importantly, the value of l_c for the second superstructure (l_{c2}) is two times that for the first one ($l_{c2} = 2l_{c1}$). The physical reason for this is that the ferroelectric layer in the immediate contact with the electrode is in a favorable position for creation of the domain structure: a part of the stray electric field associated with this structure is screened by the electrode. This is why for $l > l_{c1}$ the phase transition in the first superstucture is higher than in the second one with the same material parameters and period of the superstructure. The difference in the phase transition temperatures can considerable. For the superstructure with the parameters of $BaTiO_3-SrTiO_3$ superstructure starting from about $l = 4$ nm up to $l = 20$ nm this difference can be about 100 °C (See Figure 7). Also note that the phase transition temperature in either superstructure does not depend on number of the unit cells composing the superstructure and is the same as the phase transition temperature for a single bilayer or a single ChT cell.

Quite spectacular is the difference between the polarization profiles arising at the phase transitions into multidomain states in the two superstructures. The polarization profile in the first superstructure is very different from the periodic along the superstructure profile arising in the second superstructure (Figures 10 and 13). We see that it is incorrect to

assume periodicity along the thickness of the superstructure if this is the superstructure consisting of what we call the bilayer cells. For the second superstructure this is possible but this superstructure is very specific because it is symmetric. The origin of the periodicity is this symmetry, not the large number of the unit cells in the superstructure. The first superstructure is not symmetric and this is also the case for any real superstructure. In Sec.2 we considered, as an example, a nonsymmetrical trilayer where thickness of a paraelectric layer neighboring with an electrode is less than $l/2$ at the expence of the paraelectric layer neighboring the opposite electrode. We have seen that the maximum value of l corresponding to phase transition into a single domain structure (l_{cn}) is intermediate between l_{c1} and l_{c2}. It proved to be algebraically too laborous to consider even a two nonsymmetrical trilayer structure not to mention larger structures. It is of little doubt, however, that a superstructure having near the electrodes paraelectric layers of thickness different from $l/2$ at each oxide-electrode interface behaves qualitatively similar to the first superstructure, i. e., the profile of the polarization arising at the phase transition is not periodic along the superstructure. To be fair, let us mention that at sufficiently large l the lack of the symmetry becomes unimportant and the phase transition in a nonsymmetrical trilayer is quite similar to that in the symmetrical ChT cell. This is quite natural and means physically that formation of the domain structure in the ferroelectric layers proceeds similar to what occurs in a ferroelectric layer in an infinite paraelectric medium. Clearly, the same phenomenon is expected in superstructures with large l's where the neighbouring ferroelectric layers "do not feel each other" because intermediate paraelectric layers are too thick. Everything what we are discussing in this paper is of some real interest for superstructures with small l's. Here we mean the l's which are not very different from l_c for a given superstructure which has to be calculated, of course, with a proper account for all its specific features including the non-electrostatic boundary conditions at the interfaces and the character of the near electrode region. The latter is what is emphasized in this paper.

The parameters of this region include those of the electrodes. A real electrode can be modelled as an ideal metallic one with a dielectric "dead layer" at its surface (See, e. g., Ref. 19). It is easy to show that if the ferroelectric phase transition in the superstructure is into a single domain state these parameters of the electrode does not influence the phase transition temperature and other its characteristics. Indeed, consider a superstructure presented in Figure 15 and suppose that the phase transition is into a single domain state. Since the

electric displacement is the same through the superstructure on can see that the electric field is the same (E_f) in all the ferroelectric layers and it is also the same (E_p) in all the paraelectric ones. Therefore, we have

$$- \mid \varepsilon_f \mid E_f = \varepsilon_p E_p = \varepsilon_e E_d \tag{77}$$

The condition of the short-circuiting reads:

$$E_d d + N l_f E_f + N l_p E_p = 0. \tag{78}$$

This system of three linear equations has non-trivial solutions (point of the stabilitity loss of the paraelectric phase) if

$$\varepsilon_f = -\frac{l_f \varepsilon_p}{l_p \left(1 + \frac{d\varepsilon_p}{N\varepsilon_e}\right)} \simeq \frac{l_f \varepsilon_p}{l_p}. \tag{79}$$

For sufficiently large N the last approximate equality is almost exact even for very poor electrodes, i. e. those with large d and small ε_e. Physically this means that even the presence or absence of the electrodes is not important for the phase transition into a single domain state.

But to define conditions for a single domain transition and to find the temperature and other characteristics of a phase transition into a multidomain state one has to take into account the parameters of the electrodes as our paper convincingly shows. This is not an easy task, unfortunately, but it is natural to expect that the difference between the first and second superstructure will be less dramatic that what we have found in this paper if these superstructures are supplied with real electrodes. All in all, at this moment, we do not attempt to carry our work further to take into account the real nature of the electrodes as we think that this question deserves a seperate study.

V. CONCLUSIONS

We considered the phase transition in superstructures consisting of ferroelectric-paraelectric units having equal layer thicknesses. The case of the polar axis perpendicular to the film plane has been treated. Our aim was to find the phase transition temperature and the profile of the polarization appearing at the transition considering. To do so, we

use the phenomenological Landau-Ginzburg-Devonshire theory together with the equations of electrostatics. The effects of non-electrostatic boundary conditions have been neglected. The approach was general but to illustrate the results we referred to $BaTiO_3$-$SrTiO_3$ system. The ferroelectric phase transition in the superstructures is known to be into a multidomain state if the thickness of the layers is larger than a certain ("critical") thickness. For such transitions we showed that the transition temperature and appearing domain structures are very sensitive to the nature of the near-electrode regions. Specifically, whether electrodes are in contact with the ferroelectric layers or not has a prominent impact on these charateristics and on the value of the critical thickness. Moreover, the typical situation proved to be that the amplitude of the appearing polarization "waves" in the plane of a given layer is a function of the layer position with respect to the electrodes.This is irrespective of the number of the units in the superstructure and, therefore, the usual assumption about periodicity in superstructures with sufficiently large number of units is not justified. The periodicity is possible in a special case only when the near-electrode layers are paraelectric with half layer thickness. This is once again valid irrespective of the number of the units and is connected with a symmetry that the whole structure has in this case. There are many types of the inhomogeneous polarization distributions which should be, in principle, considered as candidates for the polarization distribution appearing at the phase transition. It proves unfeasible to find all these distributions even for small number of the units, not to mention the general case. However, we were able to find a type of the polarization distrubution which should be considered as the candidate for superstructures where one of the electrodes is in direct contact with the ferroelectric layer and the number of the units is arbitrary. The same is possible for the above mentioned symmetrical superstructure. Using physical arguments we have put forward a hypothesis that these distributions exactly appear at the phase transition in the respective superstructures. Our numerical simulations have supported this hypothesis. Note that the inherent inhomogeneity along the superstructure of the domain structures appearing at the phase transition should result in considerable smearing of the phase transtion anomalies observed in the superstructures for multidomain transitions. This smearing is not present and the structure of the near electrode region is not felt for the single domain transition expected for thicknesses lower than the critical one. It should be recalled, however, that the value of the critical thickness does depend on the structure of the near electrode region.

Acknowledgements

APL has been partially supported by The Scientific and Technological Research Council of Turkey (TÜBİTAK) through the BİDEB Program and by Ministry of Science and Education of Russian Federation (State Contract # 02.740.11.5156). IBM acknowledges the support by Turkish Academy of Sciences (TÜBA) GEBIP Program.

VI. REFERENCES

1. A. Erbil, Y. Kim and R. A. Gerhardt, Phys. Rev. Lett. **77**, 1628 (1996).
2. E. D. Specht, H. -M. Christen, D. P. Norton and L. A. Boatner, Phys. Rev. Lett. **80**, 4317 (1998).
3. D. A. Tenne, A. Bruchhausen, N. D Lanzillotti-Kimura, A. Fainstein, R. S Katiyar, A. Cantarero, A Soukiassian, V. Vaithyanathan V, J. H. Haeni, W. Tian, D. G. Schlom, K. J. Choi, D. M. Kim, C. B. Eom, H. P. Sun, X. Q. Pan, Y. L. Li, L. Q. Chen, Q. X. Jia, S. M. Nakhmanson, K. M. Rabe, X. X. Xi, Science **313**, 1614 (2006)
4. F. Fishman, F. Schwabl and D. Schenk, Phys. Lett. A **121**, 192 (1987).
5. D. R.Tilley, Sol. State Comm. **65**, 657 (1988).
6. D. Schwenk, F.Fishman, and F.Schwabl, Phys. Rev. B **38**, 11618 (1988).
7. D. Schwenk, F.Fishman, and F.Schwabl, J.Phys. Cond. Mat. **2**, 5409 (1990).
8. K. Iijima, T. Terashima, Y. Bando, K. Kamigaki, and H. Terauchi, J. Appl. Phys. **72**, 2840 (1992).
9. H. Tabata, H. Tanaka, and T. Kawai, Appl. Phys. Lett. **65**, 1970 (1994).
10. J. B. Neaton and K. M. Rabe, Appl. Phys. Lett. **82**, 1586 (2003).
11. A. L. Roytburd, S. Zhong and S. P. Alpay, Appl. Phys. Lett. **87**, 092902 (2005).
12. I. P. Batra and B. D. Silverman, Sol. Stat. Comm. **11**, 291 (1972).
13. E. V. Chensky and V.V. Tarasenko, Sov. Phys. JETP **56**, 618 (1982); Zh. Eksp. Teor. Fiz. **83**, 1089 (1982).
14. V. A. Stephanovich, I. A. Luk'yanchuk, and M. G. Karkut, Phys. Rev. Lett. **94**, 047601 (2005).
15. Y. L. Li, S.Y. Hu, D. Tenne, A. Soukiassian, D. G. Schlom, X. X. Xi, K. J. Choi,

C. B. Eom, A. Saxena, T. Lookman, Q. X. Jia, and L. Q. Chen,
Appl. Phys. Lett. **91**, 112914 (2007).

16. We present the Chensky-Tarasenko method not following their paper literally but in a somewhat modernized form. They considered a vacuum dead layer. Other authors generalized their treatment, see e.g. A. S. Sidorkin, Domain Structure in Ferroelectrics and Related Materials, Cambridge Int. Science Publishing, (2006).
17. H. Suhl, Appl. Phys. **8**, 217 (1975).
18. A. Tagantsev, Ferroelectrics **375**, 19 (2008).
19. A. M. Bratkovsky and A. P. Levanyuk, J. Comp. Theor. Nanoscience 6, 1 (2009).
20. N. A. Pertsev, A. G. Zembilgotov and A. K. Tagantsev, Phys. Rev. Lett. 80, 1988 (1998).

Figure Captions

Figure 1. (Color online) The schematic of the ferroelectric layer with thin dead layers having thickness $d/2$ at the ferroelectric-electrode interfaces. This was the system which was investigated in Ref. 13.

Figure 2. (Color online) The ChT cell with thick dead layers where each paraelectric layer is $l/2$.

Figure 3. (Color online) The comparison between the analytical result (red lines) and the numerical (solid black line) of the transition temperature (in °C) ChT cell for $\varepsilon_p = 500$. The red curves reflect the small kl and the large kl limits as given in Eqs. 22 and 30. The material parameter values used in the calculations are T_C=615°C, C=1.5x10^5 °C, g=6.2x10^{-10} m^3/F, $\varepsilon_\perp = 50$.

Figure 4. (Color online) The bilayer cell having equal thickness of the ferroelectric and the paraelectric layer.

Figure 5. (Color online) (a) Transition temperatures (in °C) as a function of layer thickness for the bilayer cell for $\varepsilon_p = 100$ (hollow diamonds), $\varepsilon_p = 500$ (dark thick line) and $\varepsilon_p = 1000$ (gray triangles) and (b) Critical k as a function of layer thickness for the bilayer cell for $\varepsilon_p = 100$ (solid line), $\varepsilon_p = 500$ (dashed line) and $\varepsilon_p = 1000$ (red line). The material parameter values used in the calculations are T_C=615°C, C=1.5x10^5 °C, g=6.2x10^{-10} m^3/F, $\varepsilon_\perp = 50$.

Figure 6. (Color online) The schematic of the non-symmetrical trilayer.

Figure 7. Comparison of (a) the numerical solutions for transition temperature for the bilayer cell (solid thick line), the non-symmetrical cell with $l/4$, $3l/4$ paraelectric layer partitioning (hollow squares) and the ChT cell (hollow triangles) (b) the k_c at the

transition for the bilayer cell (thick solid line), the asymmetrical cell (dashed line) and the ChT cell (red line) for the $BaTiO_3$-$SrTiO_3$ system. The values used for $BaTiO_3$ fully strained on $SrTiO_3$ in the calculations are T_C=615°C (Computed using the constants given in Ref. 20), C=1.5x10^5 °C, g=6.2x10^{-10} m^3/F and $\varepsilon_\perp = 20$, $\varepsilon_p = 300$ for $SrTiO_3$ and is assumed constant in the entire temperature range for convenience.

Figure 8. (Color online) The schematic where unit cells of the superstructure consisting of (a) bilayers and (b) ChT cells are shown.

Figure 9. (Color online) Two bilayer cell system mentioned in Section 3.1.

Figure 10. (Color online) The polarization profile at the temperature of loss of stability of the paraelectric phase in the superstructure consisting of 4 bilayers (blue curve) and 8 bilayers (red curve) with 5 nm and 2.5 nm layer thickness respectively. Note that the total thickness of the system in both cases is the same and fixed at 40 nm. The ferroelectric layers are $BaTiO_3$ and the paraelectric ones are $SrTiO_3$. Critical thickness for single domain state stabilization is 2.2 nm. The 5 nm layer has a much more rapidly decaying polarization along the thickness. The values used for $BaTiO_3$ in the calculations are T_C=615°C (Computed using the constants given in Ref. 20), C=1.5x10^5 °C, g=6.2x10^{-10} m^3/F and $\varepsilon_\perp = 20$, $\varepsilon_p = 300$ for $SrTiO_3$ and is assumed constant in the entire temperature range for convenience.

Figure 11. (Color online) Two ChT cell system mentioned in Section 3.3.

Figure 12. Comparison of the transition temperatures (in °C) of the two-bilayer cell (solid line), the two-ChT cell (hollow squares) and the secondary solution (hollow triangles) of the two-bilayer and the two-ChT cell as a function of layer thickness for (a) $\varepsilon_p = 100$ and (b) $\varepsilon_p = 500$. The material parameter values used in the calculations are T_C=615°C, C=1.5x10^5 °C, g=6.2x10^{-10} m^3/F, $\varepsilon_\perp = 50$.

Figure 13. (Color online) The polarization wave profile at the temperature of loss of stability of the paraelectric phase in the superstructure consisting of 3 ChT cells each layer having 8 nm thickness (blue curve) and 4 ChT cells with each layer being 5 nm thick (red curve). Critical thickness for single domain state stabilization is 4.4 nm. The values used for $BaTiO_3$ in the calculations are T_C=615°C, C=1.5x10^5 °C, g=6.2x10^{-10} m^3/F and $\varepsilon_\perp = 20$, $\varepsilon_p = 300$ for $SrTiO_3$ and is assumed constant in the entire temperature range for convenience.

Figure 14. (Color online) The polarization maps obtained in our numerical simulations 5°C below the phase transition for the $BaTiO_3$-$SrTiO_3$ system strained on a thick electroded $SrTiO_3$ substrate consisting of (a) 8 ChT cells and (b) 8 bilayers with each system having 80 nm total thickness. The system in (a) has a phase transition temperature around 150°C and the one in (b) 220°C, in very good agreement with analytical results. The perpendicular colorbar scales are for normalized polarization. The values used for $BaTiO_3$ in the calculations are T_C=615°C, C=1.5x10^5 °C, g=6.2x10^{-10} m^3/F and $\varepsilon_\perp = 20$, $\varepsilon_p = 300$ for $SrTiO_3$ and is assumed constant in the entire temperature range for convenience.

Figure 15. (Color online) The schematic of a superstructure with real electrodes (denoted by the presence of dead layers at the oxide-electrode interfaces). The electric field in the paraelectric (E_P) and in the ferroelectric (E_F) are in opposite directions to satisfy D=Constant in the system.

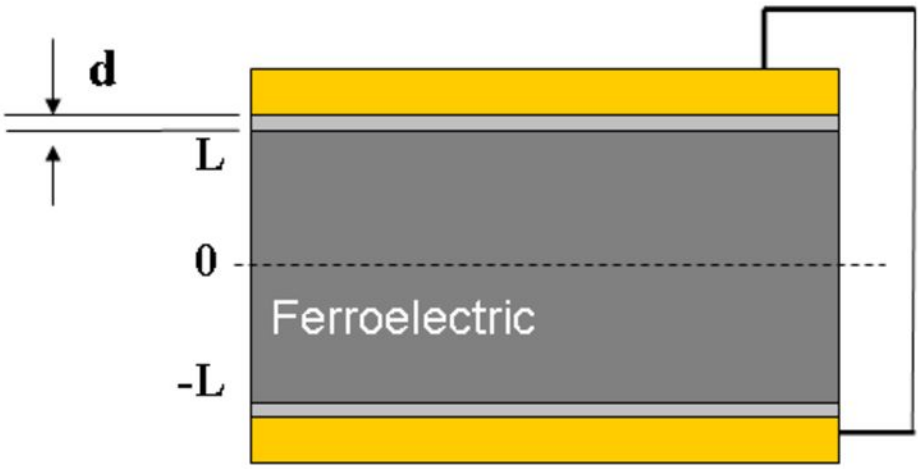

Figure 1

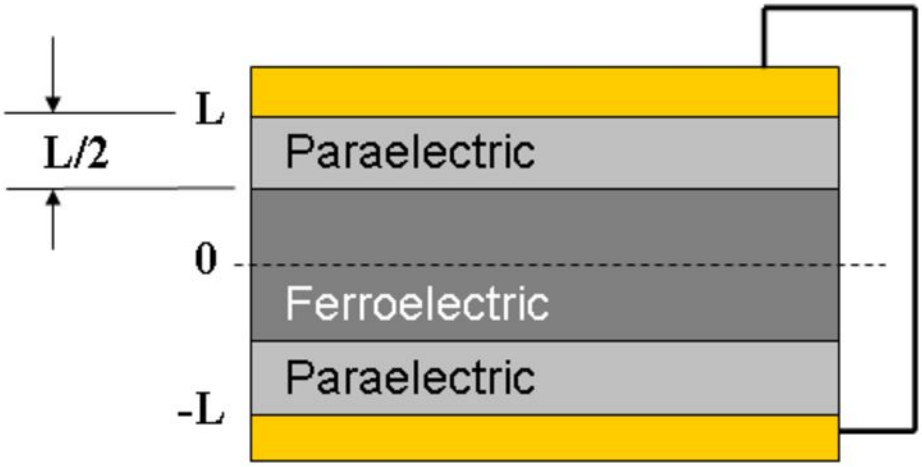

Figure 2

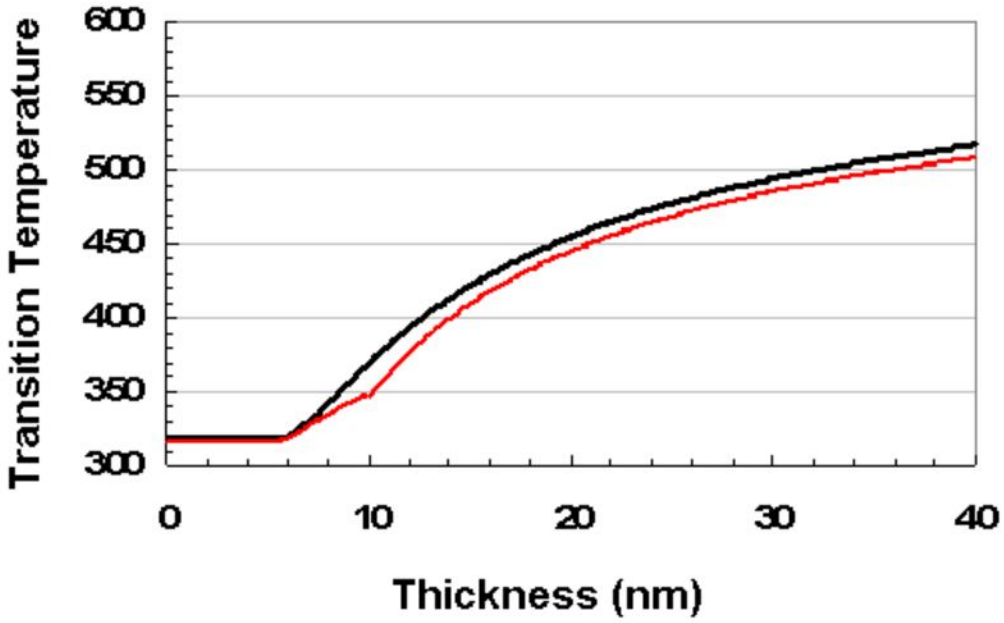
Transition Temperature
600
550
500
450
400
350
300
0
10
20
30
40
Thickness (nm)

Figure 3

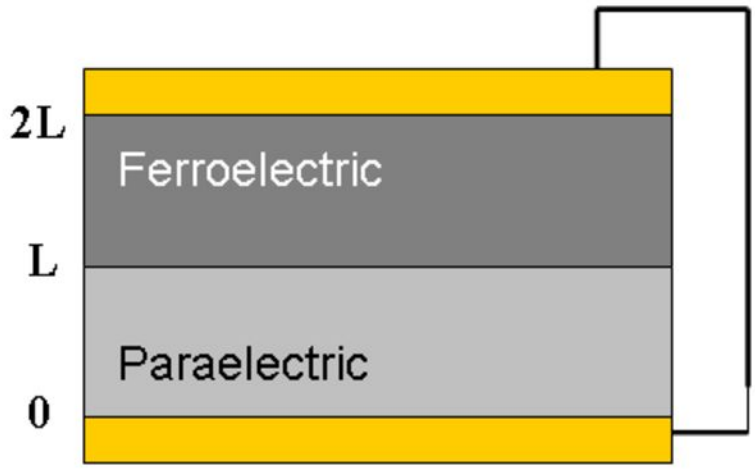

Figure 4

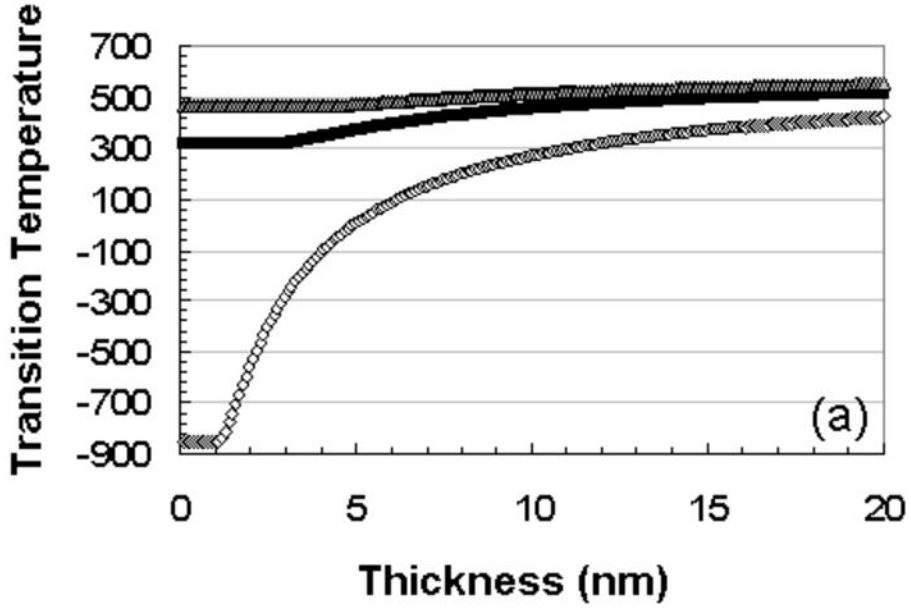
Transition Temperature
700
500
300
100
-100
-300
-500
-700
-900
0
5
10
15
20
Thickness (nm)
(a)

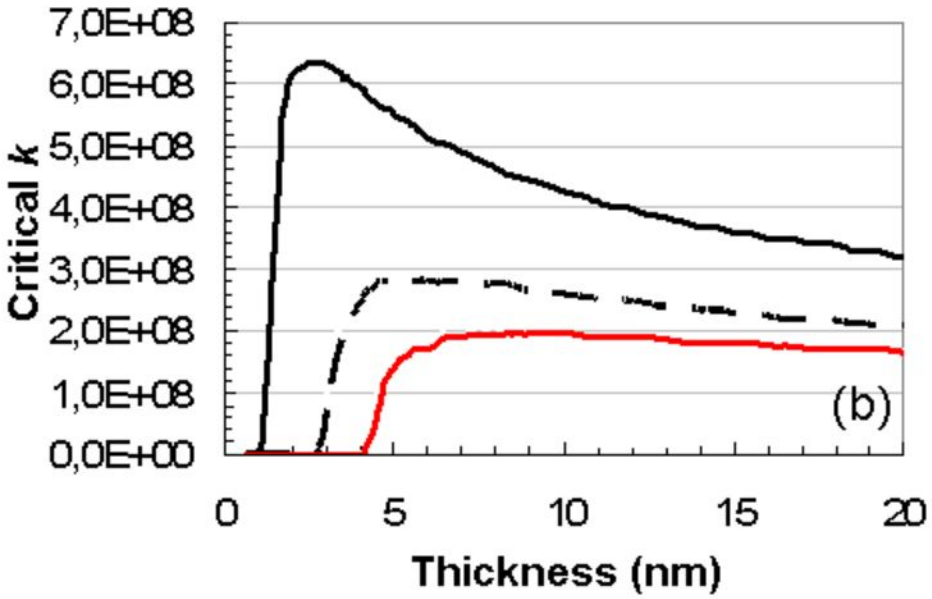
Critical k
7,0E+08
6,0E+08
5,0E+08
4,0E+08
3,0E+08
2,0E+08
1,0E+08
0,0E+00
0
5
10
15
20
Thickness (nm)
(b)

Figure 5

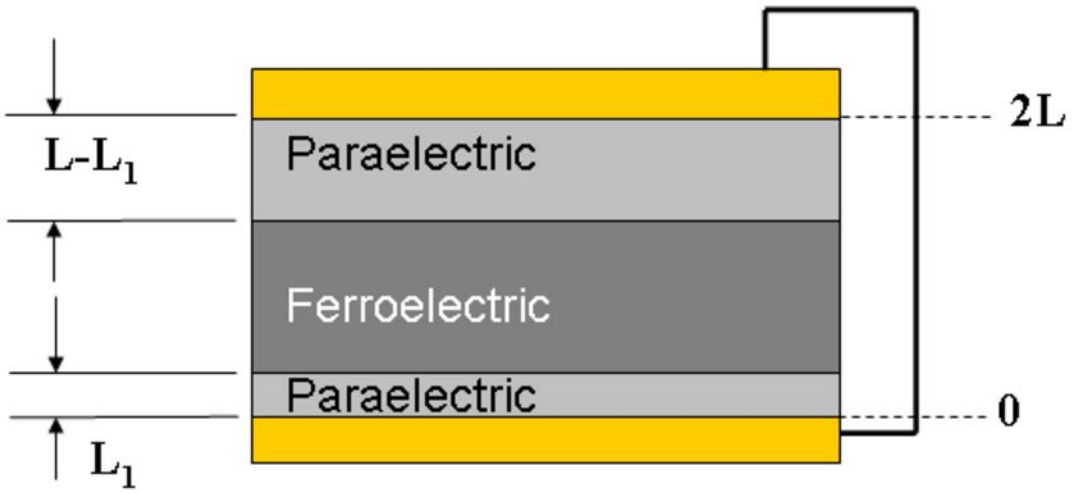

Figure 6

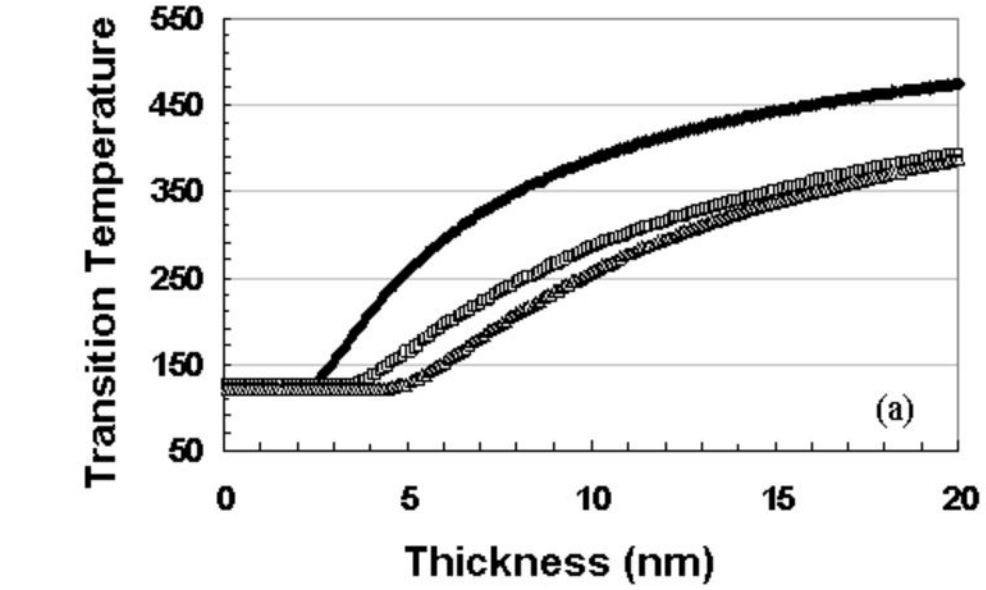
Transition Temperature
550
450
350
250
150
50
0
5
10
15
20
Thickness (nm)
(a)

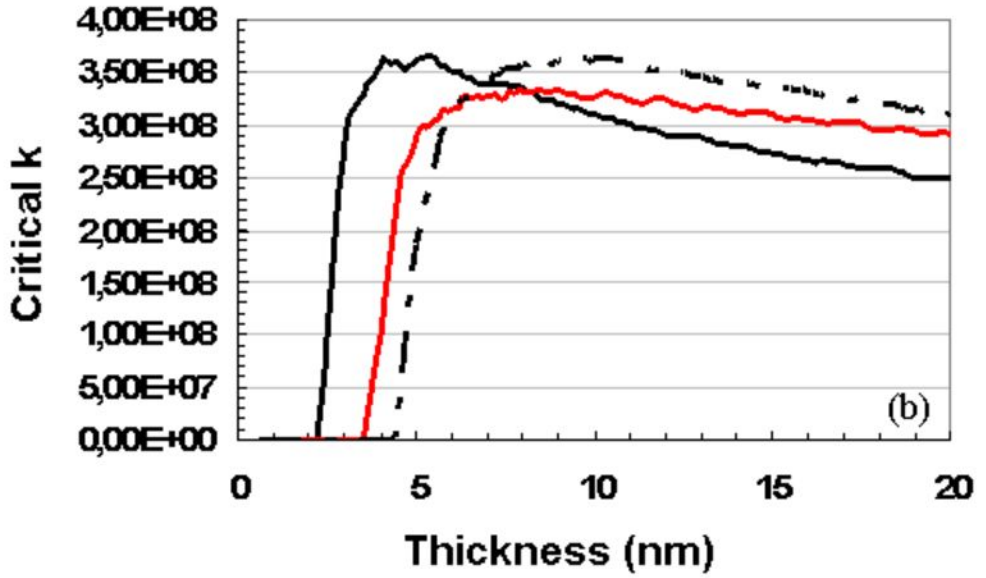
Critical k
4,00E+08
3,50E+08
3,00E+08
2,50E+08
2,00E+08
1,50E+08
1,00E+08
5,00E+07
0,00E+00
0
5
10
15
20
Thickness (nm)
(b)

Figure 7

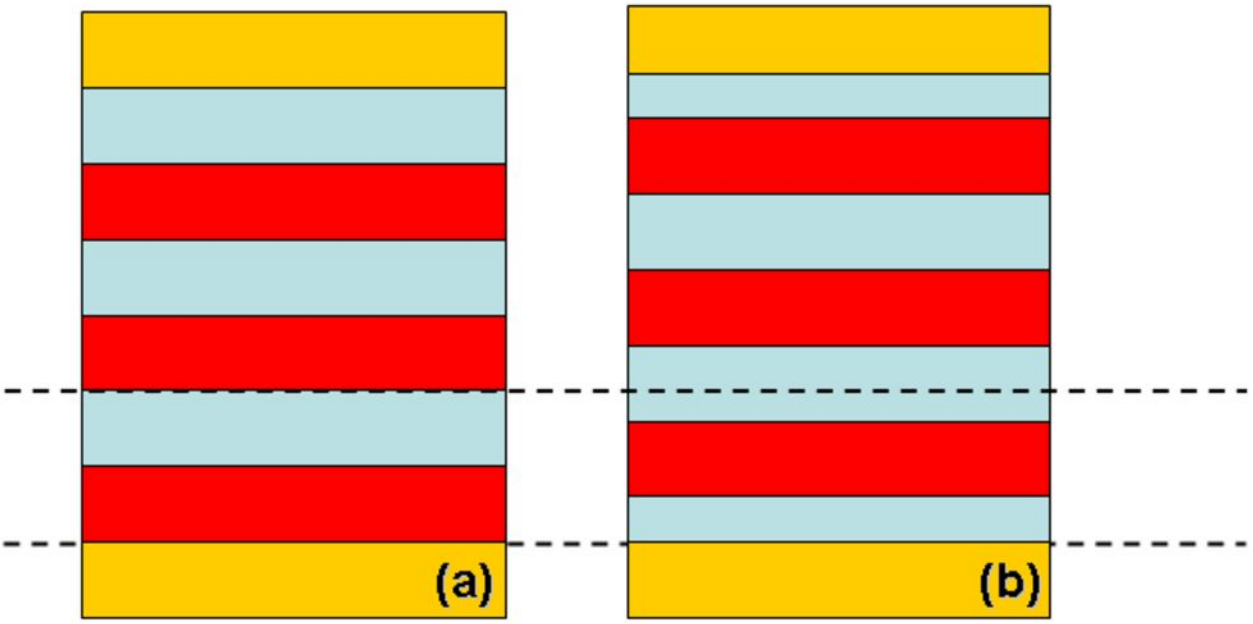

Figure 8

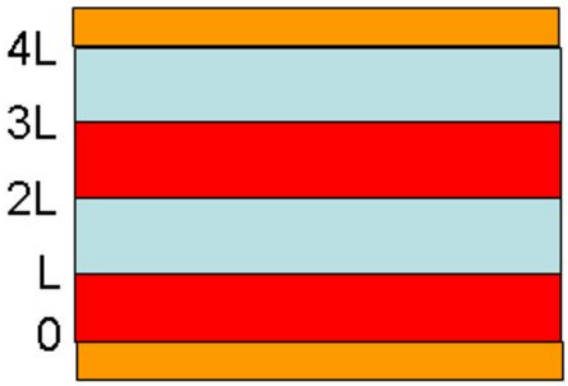

Figure 9

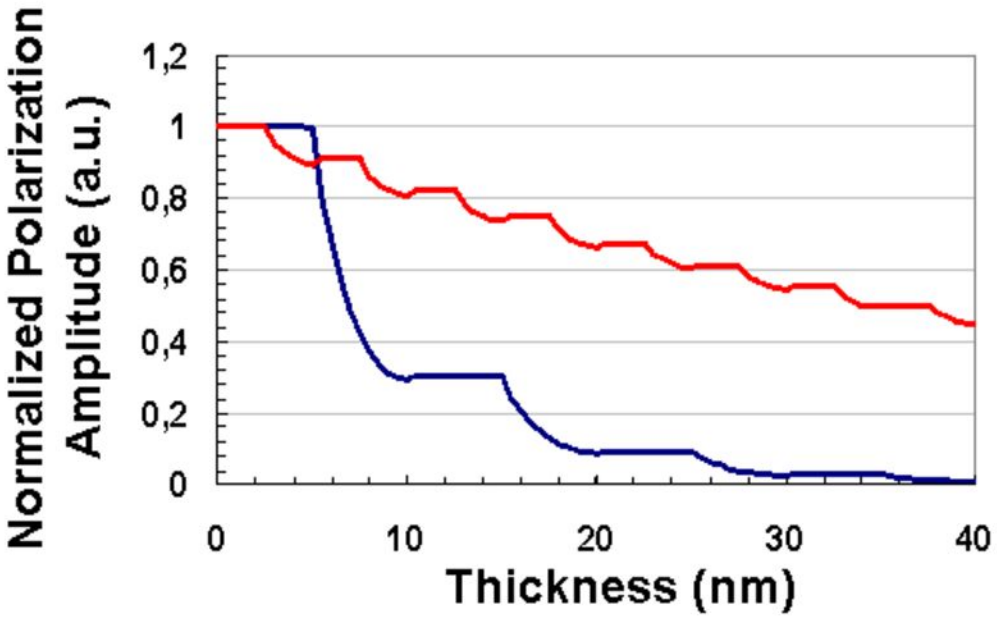
Normalized Polarization Amplitude (a.u.)
1,2
1
0,8
0,6
0,4
0,2
0
0
10
20
30
40
Thickness (nm)

Figure 10

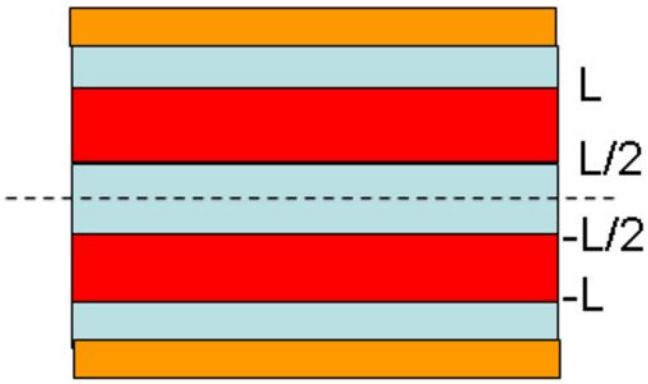

Figure 11

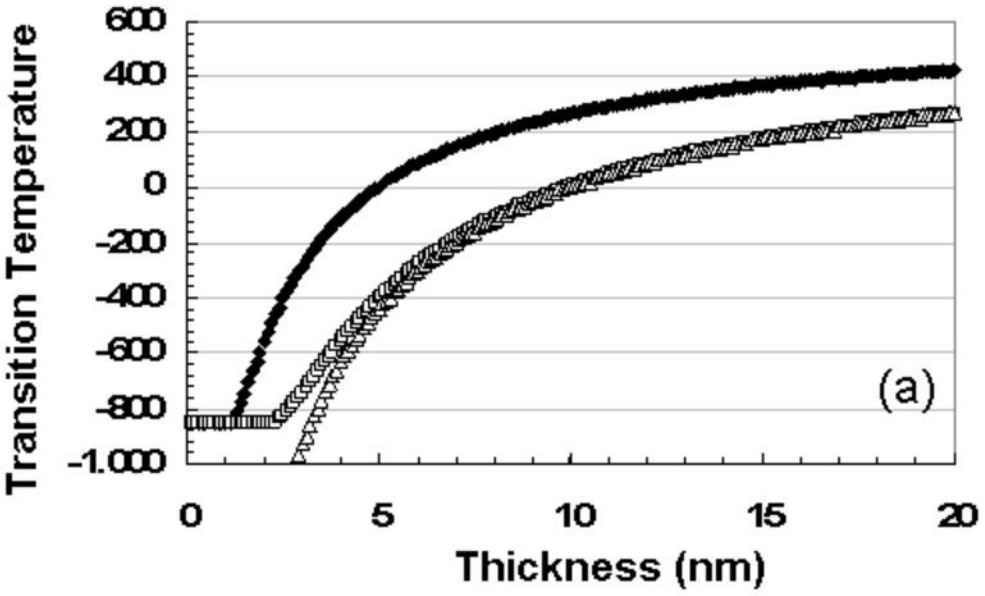
Transition Temperature
600
400
200
0
-200
-400
-600
-800
-1.000
0
5
10
15
20
Thickness (nm)
(a)

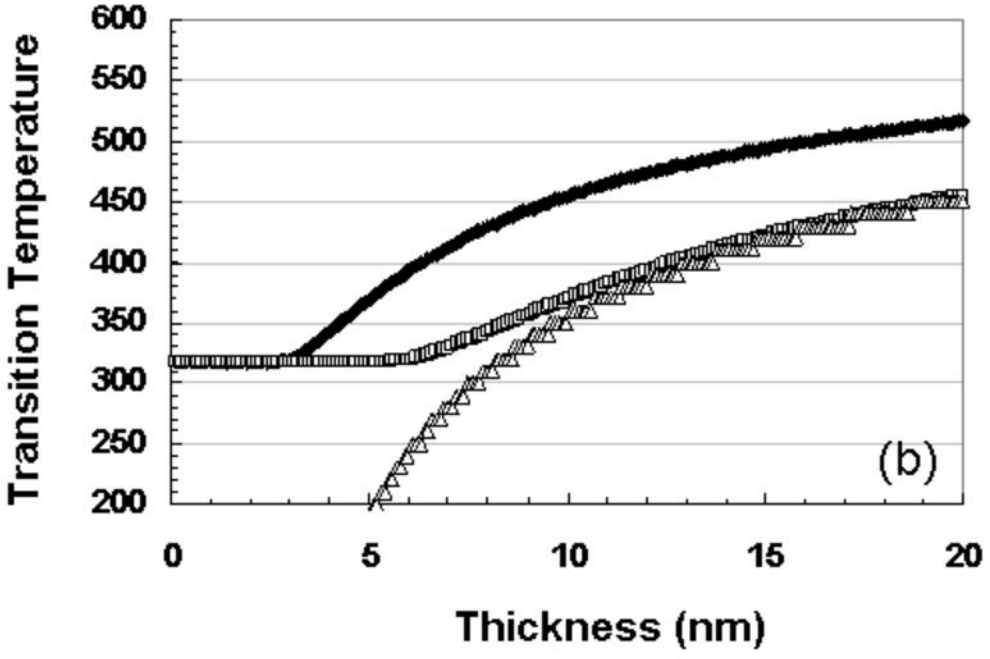
Transition Temperature
600
550
500
450
400
350
300
250
200
0
5
10
15
20
Thickness (nm)
(b)

Figure 12

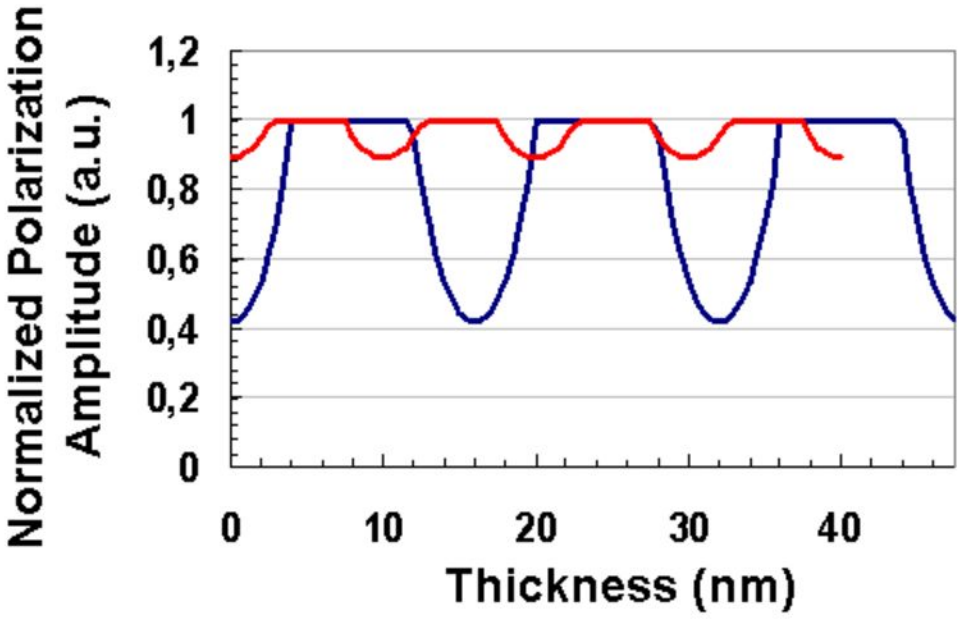
Normalized Polarization Amplitude (a.u.)
1,2
1
0,8
0,6
0,4
0,2
0
0
10
20
30
40
Thickness (nm)

Figure 13

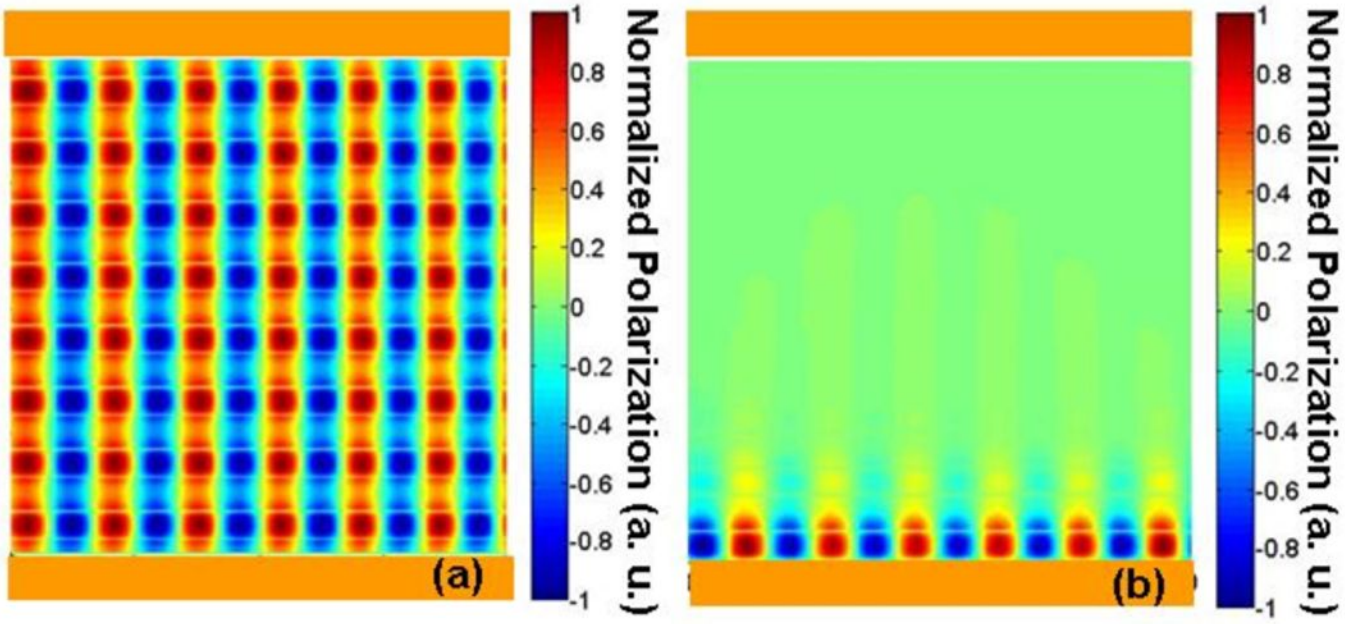
(a)
(b)
Normalized Polarization (a. u.)
Normalized Polarization (a. u.)
1
0.8
0.6
0.4
0.2
0
-0.2
-0.4
-0.6
-0.8
-1

Figure 14

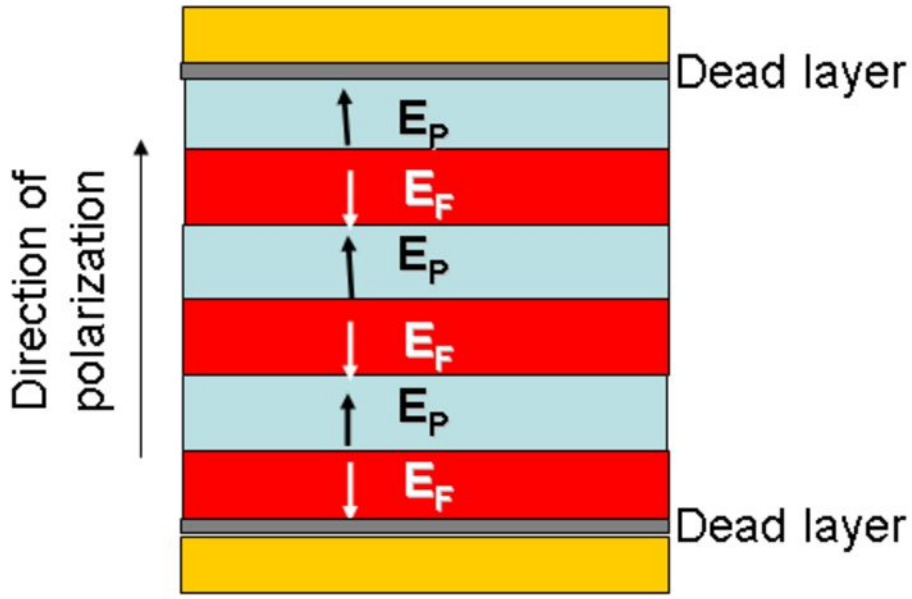
Dead layer
E_P
E_F
E_P
E_F
E_P
E_F
Dead layer
Direction of polarization

Figure 15